

AN ACCELERATION SCHEME FOR THE MULTIGROUP S_n EQUATIONS WITH FISSION AND THERMAL UPSCATTER

B. T. Adams
Interfaculty Reactor Institute
Delft University of Technology
2629 JB Delft, the Netherlands
31 (15) 278-6594

J. E. Morel
University of California
Los Alamos National Laboratory
Los Alamos, New Mexico 87545
(505) 667-6091

ABSTRACT

We have developed a three-step acceleration scheme for the outer-iterations of the multigroup S_n equations with fission and thermal neutron upscatter. Although it has only been tested in 1-D slab and 2-D rectangular geometries with linear-discontinuous and bilinear-discontinuous spatial differencing, respectively, previous experience suggests that it should be applicable in any geometry with any spatial differencing scheme for which an unconditionally efficient diffusion-synthetic acceleration scheme exists. The method is derived, theoretically analyzed, and computationally tested. Our results indicate that the scheme is unconditionally effective in terms of error reduction per iteration and highly efficient in terms of computational cost.

I. INTRODUCTION

The standard outer-iteration scheme used to solve the multigroup S_n equations is the Gauss-Seidel scheme. In the absence of upscatter reactions (i.e. reactions in which a particle gains energy), the Gauss-Seidel method yields the exact flux solution in a single iteration. However, if there is upscattering and a low probability for particle absorption or leakage, the convergence rate of this iterative process can become arbitrarily slow. To our knowledge, the only existing upscatter acceleration techniques currently in use are the group-dependent rebalance methods such as that employed in the ONETRAN¹ code. The effectiveness of these schemes is strongly problem dependent and they often fail on precisely those problems for which convergence acceleration is most needed. An unconditionally effective acceleration scheme is desired.

We have developed an acceleration scheme for the multigroup S_n equations with both fission and thermal upscatter sources. We initially derived and theoretically analyzed two alternative acceleration algorithms: a two-step algorithm which was intended to accelerate the convergence rate of the fission and thermal upscatter sources simultaneously, and a three-step algorithm which was designed to accelerate these source terms separately. Each of these alternatives could be considered as a logical extension of two previous works: the S_N fission source acceleration technique of Morel and McGhee², and the S_N thermal upscatter source acceleration scheme that we previously developed³. We selected the three-step algorithm for computational testing because our theoretical analysis indicated it was slightly more effective than the two-step algorithm. Our theoretical and computational results indicate that this scheme gives rapid convergence rates at a cost per iteration which is very little more than that of the unaccelerated scheme. Although we explicitly consider

only source calculations here, our method can also be applied in conjunction with inverse power iteration in eigenvalue calculations. This follows from the fact that each inverse power iteration requires the solution of an effective source problem.

II. THE ACCELERATED METHOD

In one-dimensional slab geometry, the multigroup transport equation for a multiplying media is given by:

$$\begin{aligned} \mu \frac{\partial \Psi_g(x, \mu)}{\partial x} + \Sigma_{t,g}(x) \Psi_g(x, \mu) &= \frac{\chi_g(x)}{4\pi} \sum_{g'=1}^G \nu_{g'}(x) \Sigma_{f,g'}(x) \Phi_{o,g'}(x) \\ &+ \sum_{l=0}^L \frac{2l+1}{4\pi} P_l(\mu) [Q_{l,g}(x) + \sum_{g'=1}^G \Sigma_{s,l,g' \rightarrow g}(x) \Phi_{l,g'}(x)] \quad , g = 1, G, \end{aligned} \quad (1)$$

where the macroscopic differential scattering cross section and angularly-dependent external source, $Q_g(x, \mu)$, have been expanded in the Legendre polynomials and standard variable notation has been utilized. The Gauss-Seidel iterative method is the standard technique for solving Eq. (1), and it can be described as follows:

$$\begin{aligned} \mu \frac{\partial \Psi_g^{k+1}(x, \mu)}{\partial x} + \Sigma_{t,g}(x) \Psi_g^{k+1}(x, \mu) &= \frac{\chi_g(x)}{4\pi} \sum_{g'=1}^G \nu_{g'}(x) \Sigma_{f,g'}(x) \Phi_{o,g'}^k(x) \\ &+ \sum_{l=0}^L \frac{2l+1}{4\pi} P_l(\mu) [Q_{l,g}(x) + \sum_{g'=1}^g \Sigma_{s,l,g' \rightarrow g}(x) \Phi_{l,g'}^{k+1}(x) + \sum_{g'=g+1}^G \Sigma_{s,l,g' \rightarrow g}(x) \Phi_{l,g'}^k(x)] \end{aligned} \quad (2)$$

where k is the iteration index and neutron downscatter and upscatter are separated. Note that, in the absence of fission and thermal upscatter, the Gauss-Seidel equations yield the exact solution in a single iterate. By subtracting Eq. (2) from Eq. (1), an exact equation for the error in the Gauss-Seidel iterate is obtained:

$$\begin{aligned} \mu \frac{\partial \epsilon_g^{k+1}(x, \mu)}{\partial x} + \Sigma_{t,g}(x) \epsilon_g^{k+1}(x, \mu) &= \frac{\chi_g(x)}{4\pi} \sum_{g'=1}^G \nu_{g'}(x) \Sigma_{f,g'}(x) \epsilon_{o,g'}^k(x) \\ &+ \sum_{l=0}^L \frac{2l+1}{4\pi} P_l(\mu) \left[\sum_{g'=1}^g \Sigma_{s,l,g' \rightarrow g}(x) \epsilon_{l,g'}^{k+1}(x) + \sum_{g'=g+1}^G \Sigma_{s,l,g' \rightarrow g}(x) \epsilon_{l,g'}^k(x) \right] \end{aligned} \quad (3)$$

where

$$\epsilon_g^{k+1}(x, \mu) = \Psi_g(x, \mu) - \Psi_g^{k+1}(x, \mu) \quad , \quad (4)$$

$$\epsilon_{g',l}^{k+1}(x) = 2\pi \int_{-1}^1 \epsilon_{g'}^{k+1}(x, \mu') P_l(x, \mu') d\mu' \quad . \quad (5)$$

The error associated with the Gauss-Seidel iterate (and hence the exact solution) can be obtained by solving this equation. However, this is not practical since this equation is no easier to solve than the exact multigroup transport equation. The central idea behind our accelerated method is to obtain an economical yet accurate estimate of the error by solving a coarse-grid approximation of this equation, which is added to the flux iterate.

We have performed infinite-medium Fourier analyses for the Gauss-Seidel iteration operators corresponding to each of several materials. Our Fourier analyses are described in a subsequent section. If our acceleration scheme is to be effective, the coarse-grid approximation to Eq. (3) must be very accurate for the persistent error modes. The Fourier analysis indicated that the most poorly attenuated error modes are nearly constant in space and nearly isotropic in angle, which suggests that a diffusion approximation can be used for the coarse-grid operator. The spectral shape of the fundamental eigenvector of the Gauss-Seidel iteration matrix for various moderator to fuel ratios (MFRs) indicated that unique one-group diffusion operators could be used to eliminate the error modes associated with the thermal upscatter and fission sources. The convergence rate of the fission and thermal upscatter sources will thus be accelerated independently using the appropriate spectral shape functions. We can expect that these operators will accurately estimate the persistent error modes. However, it is important to realize that an accurate estimate of the persistent error modes is *necessary* but not *sufficient* to ensure an effective acceleration scheme. Usually one must simply choose a coarse-grid operator based upon its accuracy for the persistent error modes, and then perform a Fourier analysis to determine its effect upon the non-persistent modes.

Our three-step acceleration scheme assumes that independent error modes exist for the fission and thermal upscatter source terms. Thus, a coarse-grid error equation must be developed for each of these sources. The error equation for the thermal upscatter source term is derived by first subtracting Eq. (2) from the exact relation of Eq. (1), *without* including the fission source term. A one-third index will be used for the Gauss-Seidel iterate, rather than the unit-index incorporated in Eq. (2), in anticipation of a three-step accelerated algorithm. Performing this manipulation, an equation for the error in the Gauss-Seidel iterate that is associated with the thermal upscatter source is obtained:

$$\mu \frac{\partial \epsilon_g^{k+\frac{1}{3}}(x, \mu)}{\partial x} + \Sigma_{t,g}(x) \epsilon_g^{k+\frac{1}{3}}(x, \mu) = \sum_{l=0}^L \frac{2l+1}{4\pi} P_l(\mu) \left[\sum_{g'=1}^G \Sigma_{s,l,g' \rightarrow g}(x) \epsilon_{l,g'}^{k+\frac{1}{3}}(x) + R_{t,l,g}^{k+\frac{1}{3}}(x) \right], \quad (6)$$

where the residual thermal source, $R_{t,l,g}^{k+\frac{1}{3}}(x)$, is given by:

$$R_{t,l,g}^{k+\frac{1}{3}}(x) \equiv \sum_{g'=g+1}^G \Sigma_{s,l,g' \rightarrow g}(x) \left[\Phi_{l,g'}^{k+\frac{1}{3}}(x) - \Phi_{l,g'}^k(x) \right]. \quad (7)$$

Eq. (6) defines the error in successive Gauss-Seidel iterates with thermal upscatter and no fission source. The accelerated thermal upscatter scheme that we previously developed is designed to increase the convergence rate of precisely these problems³. Thus, this scheme may be used directly to accelerate the convergence of the thermal upscatter source. A full derivation of this acceleration scheme is included in the reference and will not be repeated herein. We will suffice to say that we approximate Eq. (6) with the coarse-grid operator defined by the one-group diffusion equation:

$$-\overline{\nabla} \cdot \langle D(x) \rangle \overline{\nabla} E_t(x) + \langle \Sigma_a(x) \rangle E_t(x) = \langle R_t^{k+\frac{1}{3}}(x) \rangle \quad (8)$$

where

$$\begin{aligned}
\langle D(x) \rangle &\equiv \sum_{g=1}^G D_g(x) \xi_g(x) \quad , \\
\langle \Sigma_a(x) \rangle &\equiv \sum_{g=1}^G \left[\Sigma_{t,g}(x) \xi_g(x) - \sum_{g'=1}^G \Sigma_{s,o,g' \rightarrow g}(x) \xi_{g'}(x) \right] \quad , \\
\langle R_t^{k+\frac{1}{3}}(x) \rangle &\equiv \sum_{g=1}^G R_{o,g}^{k+\frac{1}{3}}(x) \quad ,
\end{aligned}$$

and the spectral weighting function, $\xi_g(x)$, is defined as the fundamental eigenvector of the P_0 Gauss-Seidel iteration matrix for an infinite medium (i.e., no leakage term) with thermal upscatter and no fission source. This calculation depends only upon the multigroup cross-section coefficients and can easily be carried out using standard mathematical library routines for each material in the problem. We solve Eq. (8) for a coarse-grid approximation to the error given by Eq. (6). The convergence rate of the iteration process is then accelerated by adding this error estimate to the Gauss-Seidel scalar flux iterate. The flux in the $(k + \frac{2}{3})$ th iterate (i.e., after the thermal upscatter diffusion correction) is thus given by the relation:

$$\Phi_{o,g}^{k+\frac{2}{3}}(x) = \Phi_{o,g}^{k+\frac{1}{3}}(x) + \epsilon_{o,g}^{k+\frac{1}{3}}(x) = \Phi_{o,g}^{k+\frac{1}{3}}(x) + E_t(x) \xi_g(x) \quad , \quad (9)$$

where $\epsilon_{o,g}^{k+\frac{1}{3}}(x)$ is the multigroup-diffusion correction obtained from a single iterate of the one-group thermal upscatter acceleration scheme.

It will be assumed that the thermal upscatter source is fully-converged by this single acceleration correction. We will show that this restriction can be relaxed in practical calculations when the scheme is computationally tested. Applying the assumption that the thermal upscatter source is fully-converged, the iterative multigroup transport equations with thermal upscatter acceleration are given by the relation:

$$\begin{aligned}
\mu \frac{\partial \Psi_g^{k+\frac{2}{3}}(x, \mu)}{\partial x} + \Sigma_{t,g}(x) \Psi_g^{k+\frac{2}{3}}(x, \mu) &= \frac{\chi_g(x)}{4\pi} \sum_{g'=1}^G \nu_{g'}(x) \Sigma_{f,g'}(x) \Phi_{o,g'}^k(x) \quad (10) \\
+ \sum_{l=0}^L \frac{2l+1}{4\pi} P_l(\mu) [Q_{l,g}(x) &+ \sum_{g'=1}^g \Sigma_{s,l,g' \rightarrow g}(x) \Phi_{l,g'}^{k+\frac{2}{3}}(x) + \sum_{g'=g+1}^G \Sigma_{s,l,g' \rightarrow g}(x) \Phi_{l,g'}^{k+\frac{2}{3}}(x)]
\end{aligned}$$

The error equation for the fission upscatter source term is derived by subtracting Eq. (10) from the exact relation of Eq. (1). This manipulation yields an equation for the error in the "thermal upscatter-accelerated" iterate associated with the fission source term:

$$\begin{aligned}
\mu \frac{\partial \epsilon_g^{k+\frac{2}{3}}(x, \mu)}{\partial x} + \Sigma_{t,g}(x) \epsilon_g^{k+\frac{2}{3}}(x, \mu) &= \frac{\chi_g(x)}{4\pi} \sum_{g'=1}^G \nu_{g'}(x) \Sigma_{f,g'}(x) \epsilon_{o,g'}^{k+\frac{2}{3}}(x) + \frac{1}{4\pi} R_{f,o,g}^{k+\frac{2}{3}}(x) \\
+ \sum_{l=0}^L \frac{2l+1}{4\pi} P_l(\mu) \sum_{g'=1}^G \Sigma_{s,l,g' \rightarrow g}(x) \epsilon_{l,g'}^{k+\frac{2}{3}}(x) \quad , \quad (11)
\end{aligned}$$

where the residual fission source, $R_{f,o,g}^{k+\frac{2}{3}}(x)$, is defined as:

$$R_{f,o,g}^{k+\frac{2}{3}}(x) \equiv \chi_g(x) \sum_{g'=1}^G \nu_{g'}(x) \Sigma_{f,g'}(x) \left[\Phi_{o,g'}^{k+\frac{2}{3}}(x) - \Phi_{o,g'}^k(x) \right] \quad (12)$$

The coarse-grid approximation to Eq. (11) is derived by first approximating the transport error equation with a multigroup diffusion equation:

$$-\vec{\nabla} \cdot D_g(x) \vec{\nabla} \epsilon_{o,g}^{k+\frac{2}{3}}(x) + \Sigma_{t,g}(x) \epsilon_{o,g}^{k+\frac{2}{3}}(x) = \chi_g(x) \sum_{g'=1}^G \nu_{g'}(x) \Sigma_{f,g'}(x) \epsilon_{o,g'}^{k+\frac{2}{3}}(x) + R_{f,o,g}^{k+\frac{2}{3}}(x) + \sum_{g'=1}^G \Sigma_{s,o,g' \rightarrow g}(x) \epsilon_{o,g'}^{k+\frac{2}{3}}(x) \quad (13)$$

It is next assumed that the solution of this error equation is given by the product of an undetermined space-dependent modulation function, $E_f(x)$, and a predetermined spectral shape function defined by the eigenvector $\alpha_g(x)$:

$$\epsilon_{o,g}^{k+\frac{2}{3}}(x) = E_f(x) \alpha_g(x) \quad , \quad (14)$$

where

$$\sum_{g=1}^G \alpha_g(x) = 1 \quad (15)$$

This spectral shape function should correspond to the spectral shape of the persistent error modes of Eq. (10). Our infinite medium Fourier analysis indicated that this shape function should correspond to the fundamental eigenvector of the P_0 Gauss-Seidel iteration matrix with the thermal upscatter term assumed to be fully converged. We initially calculated this eigenvector for each region containing a fission source, but later found that our accelerated scheme was unstable for certain multi-material problems with this approach because the moderating materials adjacent to the fuel generate large error components that are not present in the spectral weighting function used to generate the fission source coarse-grid operator. Thus, this spectral weighting function was calculated using a homogenized mixture of all the fuel and moderating materials present in the problem. Substituting from Eq. (14) into Eq. (13) and integrating over all energies (summing over all groups), the following coarse-grid equation is obtained:

$$-\vec{\nabla} \cdot \left[\langle D(x) \rangle \vec{\nabla} E_f(x) + \langle \vec{D}(x) \rangle E_f(x) \right] + \langle \Sigma_a(x) \rangle E_f(x) = \langle F(x) \rangle E_f(x) + \langle R_f^{k+\frac{2}{3}}(x) \rangle \quad (16)$$

where

$$\begin{aligned} \langle D(x) \rangle &\equiv \sum_{g=1}^G D_g(x) \alpha_g(x) \quad , \\ \langle \vec{D}(x) \rangle &\equiv \sum_{g=1}^G D_g(x) \vec{\nabla} \alpha_g(x) \quad , \\ \langle \Sigma_a(x) \rangle &\equiv \sum_{g=1}^G \left[\Sigma_{t,g}(x) \alpha_g(x) - \sum_{g'=1}^G \Sigma_{s,o,g' \rightarrow g}(x) \alpha_{g'}(x) \right] \quad , \end{aligned}$$

$$\begin{aligned} \langle F(x) \rangle &\equiv \sum_{g=1}^G \chi_g(x) \sum_{g'=1}^G \nu_{g'}(x) \Sigma_{f,g'}(x) \alpha_{g'}(x) \quad , \\ \langle R_f^{k+\frac{2}{3}}(x) \rangle &\equiv \sum_{g=1}^G R_{f,o,g}^{k+\frac{2}{3}}(x) \quad . \end{aligned}$$

Note that Eq. (16) is not a standard diffusion equation because of the term containing the gradient of the shape function. This term is identically zero in homogeneous regions, but it is non-zero in inhomogeneous regions and makes Eq. (16) incompatible with most diffusion solution techniques. Most importantly, it is mathematically undefined at material interfaces. This term is an artifact of our assumption that the spectral shape function depends only upon the material cross-sections. This is a reasonable assumption at points far from boundaries in homogeneous regions, but it is non-physical at material interfaces because it leads to a spatially discontinuous shape function. To deal with these difficulties, we simply drop the term containing the gradient of the spectral shape function. The justification for this step follows solely from the effectiveness of the resulting acceleration scheme when it is applied to inhomogeneous problems. Simplifying Eq. (16), the final form of the coarse-grid fission source error equation is obtained:

$$-\overline{\nabla} \cdot \langle D(x) \rangle \overline{\nabla} E_f(x) + \langle \Sigma_a(x) \rangle E_f(x) = \langle F(x) \rangle E_f(x) + \langle R_f^{k+\frac{2}{3}}(x) \rangle \quad . \quad (17)$$

We solve Eq. (17) for a coarse-grid approximation to the error given by Eq. (11). The convergence rate of the iteration process is then accelerated by adding this error estimate to the "thermal upscatter-accelerated" scalar flux iterate. The flux in the $(k+1)$ th iterate (i.e., after both the thermal upscatter and fission diffusion corrections) is thus given by the relation:

$$\Phi_{o,g}^{k+1}(x) = \Phi_{o,g}^{k+\frac{2}{3}}(x) + \epsilon_{o,g}^{k+\frac{2}{3}}(x) = \Phi_{o,g}^{k+\frac{2}{3}}(x) + E_f(x) \alpha_g(x) \quad . \quad (18)$$

where $\epsilon_{o,g}^{k+\frac{2}{3}}(x)$ is the multigroup-diffusion correction obtained from the one-group fission error equation. This completes one accelerated iteration. Note that only the isotropic component of the flux is being accelerated in our scheme.

III. ANALYSIS

The purpose of the Fourier analysis is to calculate the spectral radius of the Gauss-Seidel and accelerated iterative operators for one-dimensional slab geometry. An infinite homogeneous medium is assumed. To perform the analysis, the iteration equations must be manipulated to relate the flux errors prior to an iteration to the flux errors after an iteration. The differential operator that defines this relationship is called the iteration operator, and its spectral radius determines the asymptotic error reduction factor for the iteration process. The error is assumed to have a spatial dependence of the form $\exp(i\lambda x)$ for $\lambda \in (-\infty, \infty)$, where $i = \sqrt{-1}$. With this assumption, the differential operator reduces to an algebraic matrix operator, called the Fourier matrix, that depends upon the Fourier mode parameter λ . The dimensions of the Fourier matrix are determined by the number of fission neutron groups present in the cross section library and the order of the Legendre expansion of the cross sections, L . The eigenvalues of the Fourier matrix are the eigenvalues of the iteration operator that correspond to the spatial Fourier mode defined by λ . Standard library routines can

be used to compute these eigenvalues for any value of λ . We define the modal spectral radius as the spectral radius corresponding to a specific Fourier mode. The spectral radius of the iteration operator is then simply the maximum of the modal spectral radii.

The Fourier analysis was performed for infinite homogeneous slabs composed of varying mixtures of uranium dioxide fuel and heavy water, beryllium oxide, and light water moderators. The uranium was enriched to 8 atom percent in the fissile isotope U^{235} . A 69-group LANL neutron cross section library with 42 thermal upscatter groups was used in each case.⁴ The spectral radii of the Gauss-Seidel and accelerated iterative operators with isotropic scattering are given for each material in Table I. The Gauss-Seidel and three-step accelerated methods are denoted in this Table by GS and TSA, respectively. We have determined by extensive numerical evaluation that the modal spectral radius is a monotonically decreasing, even function of λ for both iterative operators; therefore, the spectral radius of these operators corresponds to the $\lambda = 0$ Fourier mode. The modal spectral radii of the accelerated scheme are smaller than or equal to the corresponding radii of the Gauss-Seidel operator in each material. This indicates that our acceleration scheme effectively attenuates the persistent error components and error amplification of the less-resilient error modes does not occur. We analyzed the spectral radius of each method for the linearly anisotropic case and found no significant differences from the isotropic case. Consequently, we elected to accelerate only the isotropic component of the flux in our accelerated schemes. Referring to Table I, the moderator to fuel ratio of the material has a significant effect on the predicted spectral radius of the Gauss-Seidel method. Note that the spectral radius of the Gauss-Seidel operator is very close to unity for infinite media composed of pure fuel and for the moderated systems that are either near criticality or severely over-moderated. The spectral radii of our accelerated operator are significantly smaller in these materials, which indicates that the computational effort required to solve the multigroup transport equations in these materials will also be significantly reduced.

IV. COMPUTATIONAL RESULTS

All calculations were performed on a Cray-YMP computer and considered a fixed source in one-dimensional slab geometry. A 69-group cross section library with P_3 scattering and 42 upscatter groups was used in each case.⁴ The spatial differencing of both the multigroup transport equation and the one-group diffusion equations was performed using a linear-discontinuous (LD) approximation. A S_4 approximation with a Gauss-Legendre quadrature set was utilized for the transport equation. A point-wise relative scalar flux convergence tolerance of 10^{-4} was used for both the inner (within-group) and outer (upscatter) iterations. The first four cases consider infinite homogeneous media composed of enriched uranium dioxide fuel alone and combined in various mixtures with heavy water, beryllium oxide, and light water moderators. These calculations correspond to the following problem:

- spatially-constant, isotropic distributed source in energy group 1
- reflective boundary conditions at left and right slab faces
- ten (10) spatial cells
- slab thickness of ten (10) spectrum-averaged mean free paths (mfp), where such a mfp is equal to three times the one-group diffusion coefficient defined by Eq. (16).

The fifth test case simulates a fuel lattice composed of seven separate regions corresponding to the fuel pellet (UO_2), the cladding (Stainless Steel), the moderator (D_2O), the inner and outer coolant channel walls (Stainless Steel), the coolant (H_2O), and a reflector (BeO). The specified problem geometry is illustrated in Figure 1. One spatial cell is utilized for each of the regions

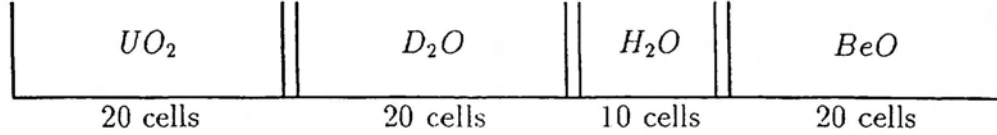


Figure 1: Spatial Geometry for Test Case 5

composed of stainless steel. This calculation corresponds to the following problem:

- isotropic surface source in energy group 1 on right face (BeO)
- reflective boundary conditions at left face (UO_2)
- cell thickness of one-tenth of a spectrum-averaged mfp.

The spectral radius of the Gauss-Seidel and accelerated fission and thermal upscatter methods for these calculations is computationally estimated as:

$$\rho = \left[\frac{\sum_{all\ i,g} (\phi_{i,g}^K - \phi_{i,g}^{K-1})^2}{\sum_{all\ i,g} (\phi_{i,g}^{K-1} - \phi_{i,g}^{K-2})^2} \right]^{\frac{1}{2}}, \quad (19)$$

where $\phi_{i,g}^k$ denotes the scalar flux iterate at step (k) for spatial cell i and energy group g , and K denotes the index for the *last* iterate.

The performance of our accelerated scheme is compared with the Gauss-Seidel scheme in Table I. The computational spectral radii of the Gauss-Seidel method show excellent agreement with theory. The spectral radii of the accelerated scheme exhibit this same agreement for the cases moderated with heavy water and beryllium oxide, but the computational spectral radii for the system moderated with light water deviate slightly from the theoretical predictions because the *first and second largest* eigenvalues of the accelerated iteration matrix are complex conjugates for the water moderated system. This characteristic resulted in the computed spectral radii of the light water system oscillating between two distinct values, rather than converging to a single value. The spectral radius of the unmoderated system is actually less than the theoretical prediction. The spectral radius of the accelerated scheme is significantly reduced relative to the Gauss-Seidel spectral radii for each case considered. Thus, effective acceleration has been obtained for these problems. The accelerated scheme is much more effective than the Gauss-Seidel method for the systems composed of pure fuel and for the moderated systems with either intermediate or high MFRs. For example,

the Gauss-Seidel scheme requires 7798, 6185, and 552 iterations for the systems with intermediate MFRs of heavy water, beryllium oxide, and light water, respectively, but our accelerated scheme requires less than 15 iterations for each of these calculations. The acceleration achieved with our scheme for low MFRs is nominal. The Gauss-Seidel method is effective for these materials, however, so significant acceleration is not required. We tested our acceleration for a multitude of MFRs and, in each case, effective acceleration was obtained when it was needed.

The fifth test case is intended to demonstrate the validity of the accelerated fission and thermal upscatter algorithm for problems containing multiple materials. The TSA scheme is faster than the standard Gauss-Seidel method by a factor of 3 for this test cases. The TSA computational spectral radius obtained for the multiple region problem is less than the maximum of the spectral radii obtained in the homogeneous problems for each material. Other inhomogeneous problems that were performed show similar behavior. The spectral radius of our accelerated scheme in multiregion problems appears to be bounded by the maximum of the spectral radii obtained in the corresponding homogeneous infinite medium problems. Thus, it would appear that the decision to neglect the drift term in the one-group diffusion equations is justified.

V. CONCLUSIONS

Our theoretical and computational results indicate that the three-step acceleration scheme is a vastly superior technique for solving the multigroup transport equations with upscatter, in comparison to the standard Gauss-Seidel technique. The degree of improvement that is obtained with our scheme is problem dependent; a significant improvement was obtained for intermediate and high MFRs, while the acceleration obtained in low MFR systems was nominal. Significant acceleration is not required for the low MFR cases, however, because the Gauss-Seidel method is quite effective in these systems.

The three-step acceleration scheme has been developed for one-dimensional slab geometry in this paper, but it appears that the method can be easily generalized to curvilinear and multidimensional geometries. We have tested the algorithm for two-dimensional rectangular geometry using a bilinear-discontinuous differencing scheme for the transport and diffusion equations.⁵ These computational results indicate that our acceleration scheme is equally effective for this geometry. An efficient implementation of our acceleration scheme requires an efficient technique for solving the coarse-grid diffusion equation. The stability of our method was preserved in our calculations by maintaining consistency in the spatial differencing of the S_n and diffusion equation. A consistently differenced diffusion equation cannot always be obtained for multidimensional S_n calculations with advanced (LD or LD-like) differencing. Furthermore, if such an equation is obtained, one may not be able to solve it efficiently. These considerations may limit the applicability of the three-step method for multidimensional geometries in the immediate future. However, advances in multidimensional diffusion-synthetic acceleration techniques are rapidly being made, and such advances are directly applicable to our scheme.

ACKNOWLEDGEMENTS

This work was performed under the auspices of the U.S. Department of Energy.

References

1. T. R. Hill. "ONETRAN: A Discrete Ordinates Finite Element Code for the Solution of the One-Dimensional Multigroup Transport Equation." LA-5990-MS. Los Alamos National Laboratory (1975).
2. J. E. Morel and J. M. McGhee. "A Fission-Source Acceleration Technique for Time-Dependent Even-Parity S_N Calculations." *Nucl. Sci. Eng.*, **116**, 73 (1994).
3. B. T. Adams and J. E. Morel. "A Two-Grid Acceleration Scheme for the Multigroup S_N Equations with Neutron Upscattering." *Nucl. Sci. Eng.*, **115**, 253 (1993).
4. R. E. MacFarlane. "TRANSX-CTR: A Code for Interfacing MATXS Cross-Section Libraries to Nuclear Transport Codes for Fusion-System Analysis." Los Alamos National Laboratory report LA-9863-MS (February 1984).
5. Morel, J. E., Dendy, J. E., Jr., and Wareing, T. A., "Diffusion Accelerated Solution of the Two-Dimensional S_N Equations with Bilinear-Discontinuous Differencing". *Nucl. Sci. Eng.*, **115**, 1993.

Table I: Performance of Gauss-Seidel and TSA Methods

Iterative Scheme	Material	Fourier ρ	Computed ρ	Iterations Required	CPU Time (s)
GS	UO_2	0.9953	0.9954	1,990	4,273.3
TSA	UO_2	0.1156	0.0927	8	18.1
GS	D_2O & UO_2 , 3:1 MFR	0.4665	0.4665	15	33.4
TSA	D_2O & UO_2 , 3:1 MFR	0.1881	0.1881	8	18.1
GS	D_2O & UO_2 , 37:1 MFR	0.9988	0.9988	7,798	16,721.2
TSA	D_2O & UO_2 , 37:1 MFR	0.4053	0.4053	8	18.2
GS	D_2O & UO_2 , 40,000:1 MFR	0.9999	0.9999	225,132	482,743.4
TSA	D_2O & UO_2 , 40,000:1 MFR	0.4829	0.4829	7	16.1
GS	BeO & UO_2 , 3:1 MFR	0.4710	0.4710	18	40.0
TSA	BeO & UO_2 , 3:1 MFR	0.3122	0.3122	10	22.6
GS	BeO & UO_2 , 82:1 MFR	0.9985	0.9985	6,185	13,710.3
TSA	BeO & UO_2 , 82:1 MFR	0.5674	0.5674	11	24.8
GS	BeO & UO_2 , 5,000:1 MFR	0.9987	0.9986	6,801	14,709.4
TSA	BeO & UO_2 , 5,000:1 MFR	0.5913	0.5913	14	31.3
GS	H_2O & UO_2 , 3:7 MFR	0.6405	0.6404	24	53.1
TSA	H_2O & UO_2 , 3:7 MFR	0.1475	0.1472	8	18.1
GS	H_2O & UO_2 , 4:1 MFR	0.9834	0.9834	552	1,191.2
TSA	H_2O & UO_2 , 4:1 MFR	0.2864	0.4614	9	20.3
GS	H_2O & UO_2 , 100:1 MFR	0.9921	0.9921	1,168	2,510.2
TSA	H_2O & UO_2 , 100:1 MFR	0.3312	0.3616	11	24.7
GS	7 Region	N/A	0.8450	59	810.6
TSA	7 Region	N/A	0.4522	17	238.3